

UC Davis

UC Davis Previously Published Works

Title

Biosynthesis and Regulation of Sulfomenaquinone, a Metabolite Associated with Virulence in *Mycobacterium tuberculosis*

Permalink

<https://escholarship.org/uc/item/0vn212hf>

Journal

ACS Infectious Diseases, 2(11)

ISSN

2373-8227

Authors

Sogi, Kimberly M
Holsclaw, Cynthia M
Fragiadakis, Gabriela K
[et al.](#)

Publication Date

2016-11-11

DOI

10.1021/acsinfecdis.6b00106

Peer reviewed



HHS Public Access

Author manuscript

ACS Infect Dis. Author manuscript; available in PMC 2017 November 11.

Published in final edited form as:

ACS Infect Dis. 2016 November 11; 2(11): 800–806. doi:10.1021/acsinfecdis.6b00106.

Biosynthesis and Regulation of Sulfomenaquinone, a Metabolite Associated with Virulence in *Mycobacterium tuberculosis*

Kimberly M. Sogi[†], Cynthia M. Holsclaw^{§,||}, Gabriela K. Fragiadakis[†], Daniel K. Nomura[⊥], Julie A. Leary^{||}, and Carolyn R. Bertozzi^{†,‡,*}

[†]Department of Chemistry, Stanford University, 380 Roth Way MC: 5080 Stanford, California 94305, United States

[‡]Howard Hughes Medical Institute, Stanford University, 380 Roth Way MC: 5080 Stanford, California 94305, United States

[§]Campus Mass Spectrometry Facilities, University of California, Davis, 9 Hutchison Hall, One Shields Avenue, Davis, California 95616, United States

^{||}Department of Molecular and Cellular Biology, University of California, Davis, 9 Hutchison Hall, One Shields Avenue, Davis, California 95616, United States

[⊥]Department of Nutritional Science and Toxicology, University of California, Berkeley, 127 Morgan Hall, Berkeley, California 94720, United States

Abstract

Sulfomenaquinone (SMK) is a recently identified metabolite that is unique to the *Mycobacterium tuberculosis* (*M. tuberculosis*) complex and is shown to modulate its virulence. Here, we report the identification of the SMK biosynthetic operon that, in addition to a previously identified sulfotransferase *stf3*, includes a putative cytochrome P450 gene (*cyp128*) and a gene of unknown function, *rv2269c*. We demonstrate that *cyp128* and *stf3* are sufficient for the biosynthesis of SMK from menaquinone and *rv2269c* exhibits promoter activity in *M. tuberculosis*. Loss of *Stf3* expression, but not that of *Cyp128*, is correlated with elevated levels of menaquinone-9, an essential component in the electron-transport chain in *M. tuberculosis*. Finally, we showed in a mouse model of infection that the loss of *cyp128* exhibits a hypervirulent phenotype similar to that in previous studies of the *stf3* mutant. These findings provide a platform for defining the molecular basis of SMK's role in *M. tuberculosis* pathogenesis.

Graphical abstract

*Corresponding Author: bertozzi@stanford.edu.

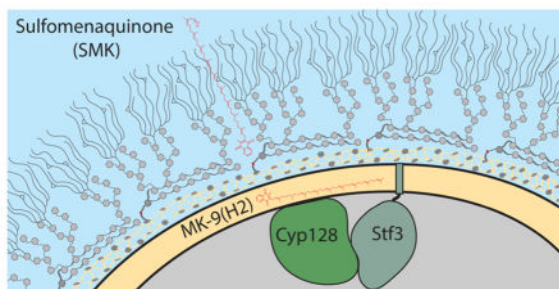
Present Addresses

(K.M.S.) School of Public Health, University of California, Berkeley, 188 Li Ka Shing, Berkeley, California 94720, United States. (B.K.F.) Department of Microbiology and Immunology, Stanford School of Medicine, Stanford University, 318 Campus Drive, Stanford, California 94305, United States.

The authors declare no competing financial interest.

Supporting Information

The Supporting Information is available free of charge on the ACS Publications website at DOI: 10.1021/acsinfecdis.6b00106. Validation of *cyp128* deletion, TLC of radiolabeled sulfated compound from WT and mutants strains, structure of menaquinone-9, schematic of *M. tuberculosis* electron transport chain with inhibitors tested, MIC values for inhibitors of cell wall biosynthesis, and plasmids and primers used in the study (PDF)



Keywords

Mycobacterium tuberculosis; menaquinone; cell wall; cytochrome P450; lipids; mass spectrometry

Mycobacterium tuberculosis has a unique cell envelope composed of multiple distinct lipid layers outside of the plasma membrane. The complex lipids in the *M. tuberculosis* cell wall serve multiple roles in bacteria. It is an effective protective barrier against oxidative and osmotic stress.¹ Many of the lipids have been shown to modulate the host immune response.^{2,3} Furthermore, bacterial lipid synthesis alleviates the toxicity from the degradation of cholesterol and odd-chain fatty acids.^{4,5} With the aid of high-resolution mass spectrometry, we are discovering the range and complexity of lipids produced by *M. tuberculosis*. It has been very challenging to identify the function and regulation of the lipids. Accordingly, defining a lipid's biosynthetic pathways is a crucial first step toward elucidating its role in *M. tuberculosis* pathogenesis.

Previous work from our laboratory identified and structurally characterized a novel sulfated lipid metabolite in *M. tuberculosis*, which we initially named S881 on the basis of its mass.^{6,7} Using mass spectrometry, we characterized the structure of S881 as an unprecedented terminally sulfated menaquinone.⁸ We renamed S881 as sulfomenaquinone (SMK), which is more descriptive of its structure. To date, SMK is the only reported example of a sulfated menaquinone derivative in any organism. SMK was discovered in a screen of *M. tuberculosis* sulfotransferase mutants. We found that the disruption of the sulfotransferase *stf3* (*stf3*) resulted in a loss of this metabolite, indicating that *stf3* was required for SMK biosynthesis. Intriguingly, the *stf3* mutant strain exhibited hypervirulence in a mouse infection model, one of the first examples of this highly unusual phenotype. The *stf3*-infected mice had an increased time to death compared to those infected with the wild-type (WT) *M. tuberculosis* strain. Although the *stf3* mutant showed no growth phenotype in vitro, mice infected with the *stf3* mutant had higher CFU in the lungs compared to WT.^{6,9}

Elucidating the machinery underlying SMK biosynthesis is an important first step toward understanding its role in *M. tuberculosis* pathogenesis. To this end, we analyzed the *M. tuberculosis* genomic region surrounding *stf3*. We observed a predicted operon that contains three genes: *stf3* (*rv2267c*), *cyp128* (*rv2268c*, a putative cytochrome P450), and *rv2269c* (a conserved hypothetical protein)¹⁰ (Figure 1A). We propose that the biosynthetic pathway for

SMK involves the hydroxylation of menaquinone, a reaction type commonly mediated by P450 enzymes, followed by Stf3-mediated sulfation (Figure 1B).

In this report, we demonstrate that *cyp128* is essential to SMK biosynthesis in *M. tuberculosis* and in *Mycobacterium smegmatis* strains engineered to produce SMK de novo. In *M. tuberculosis*, the disruption of either *stf 3* or *cyp128* results in the loss of SMK production, as determined by mass spectrometry and radiolabeling analysis. We found that the steady-state level of menaquinone is higher in the *stf 3* mutant than in WT, but no such difference was observed in the *cyp128* mutant. We hypothesized that changes in SMK and menaquinone levels would affect bacterial respiration and overall growth fitness. SMK mutants were similarly susceptible to electron-transport chain inhibitors as WT. Although SMK production had no effect on bacterial growth or respiration in vitro, levels of SMK appear to be regulated both transcriptionally and by active transport to the bacterial surface. In the mouse model of infection, we compared the *cyp128* mutant to the *stf 3* mutant and their respective complemented strains. We found that the *cyp128* mutant has increased growth in the lungs of mice compared to WT, further suggesting that SMK plays a role in host immune modulation.

RESULTS AND DISCUSSION

In the proposed operon that includes *stf 3*, which is required for the production of SMK,⁶ there are two additional genes: *rv2269c*, previously annotated as a protein of unknown function, and *cyp128*, a putative cytochrome P450 (Figure 1A). To establish whether *cyp128* and *rv2269c* are also necessary for SMK biosynthesis, we engineered *M. smegmatis*, a fast-growing relative of *M. tuberculosis*, to express the genes in various combinations. Like most mycobacteria, *M. smegmatis* utilizes menaquinone as a respiratory cofactor^{11,12} but does not encode homologues for any of the genes in the *stf 3* operon. We introduced *rv2269c*, *cyp128*, or *stf 3* individually; *cyp128* and *stf 3* only; or the entire *stf 3* operon (*rv2269c*, *cyp128*, and *stf 3*) into *M. smegmatis* on an episomal plasmid with a constitutive promoter (Table S2). To assess SMK production, total lipid extracts from all strains were analyzed by high-resolution mass spectroscopy. As expected, WT *M. smegmatis* and the strains expressing each gene individually did not produce SMK (Figure 2A and Figure S1). By contrast, the *M. smegmatis* strains expressing the entire *stf 3* operon or *cyp128* and *stf 3* together produced SMK (Figure 2A and Figure S1). We confirmed the identity of the corresponding SMK ion by fragmentation analysis as previously reported.⁸ Thus, we conclude that SMK biosynthesis from menaquinone requires only two genes, *cyp128* and *stf 3* in *M. smegmatis*. Furthermore, because the addition of *rv2269c* to *M. smegmatis* did not influence SMK production, we hypothesize that *rv2269c* is indispensable to SMK biosynthesis in *M. smegmatis*. All attempts to biochemically characterize Cyp128 and Stf3 proved unsuccessful because we were unable to express full-length soluble protein in either *E. coli* or *M. smegmatis*.

After determining that *cyp128* and *stf 3* are sufficient for SMK biosynthesis in *M. smegmatis*, we made a *cyp128* gene deletion mutant in *M. tuberculosis* strain H37Rv (*cyp128*) (Figure S2). Total lipid extracts from the *cyp128* mutant did not contain SMK as determined by high-resolution mass spectrometry (Figure 2B and Figure S4). For

comparison, total lipid extracts of the previously characterized *stf 3* mutant⁶ were made in parallel and similarly showed a loss of SMK. The complementation of *cyp128* (*cyp128::cyp128*) with WT *cyp128* restored SMK production. The loss of SMK in *cyp128* was further confirmed by growing the SMK mutants (*cyp128* and *stf 3*) on radioactive ³⁵S-containing sulfate (Figure S3A). WT, *cyp128*, *cyp128::cyp128*, and *stf 3* strains were incubated overnight in the presence of ³⁵S-sulfate in PBS, and total lipid extracts were analyzed by thin-layer chromatography (TLC). The *cyp128* and *stf 3* mutants did not produce a spot corresponding to SMK, but complementation with each respective gene restored SMK production (Figure S3A). In addition to *cyp128*, there is another cytochrome (*cyp124*) adjacent to *stf 3* in the *M. tuberculosis* genome that has been shown to have activity on structures similar to SMK in vitro.¹³ Our data confirms the role of *cyp128* in SMK biosynthesis and suggests that Cyp128 is the only cytochrome P450 of the 20 encoded in the *M. tuberculosis* genome involved in this pathway.

In addition to *cyp128* and *stf 3*, there is a small 333 bp predicted ORF *rv2269c* of unknown function.¹⁰ Bioinformatic analysis of this ORF shows very little secondary structure and no homology to any known protein. We demonstrated that *rv2269c* is not required for SMK biosynthesis in *M. smegmatis* (Figure 2A). One study of transcriptional start site mapping indicates that there is a predicted transcriptional start site of 28 nucleotides before the annotated start site of *cyp128*.¹⁴ We hypothesized that *rv2269c* is not a functional coding gene but may play a regulatory role in SMK biosynthesis. To determine if it had promoter activity, we made a series of plasmids that encoded *cyp128* along with potential promoter sequences: either one kilobase (kb) of DNA upstream of *rv2269c* (P_{nat}), 1 kb upstream of *cyp128* (including the gene *rv2269c*, $P_{nat+rv2269c}$), or the 333 bp of the *rv2269c* DNA sequence alone ($P_{rv2269c}$) (depicted in Figure S5). We transformed each of these plasmids into *cyp128* and examined the ability of each of these constructs to restore SMK production by mass spectrometry. Complementation using the promoter $P_{rv2269c}$ successfully restored SMK production in the *cyp128* mutant, whereas P_{nat} (lacking the *rv2269c* sequence) did not (Figure 3A and Figure S6). The expression of *cyp128* by the promoter $P_{nat+rv2269c}$ produced an ion with the same nominal mass as SMK, but this could not be confirmed by fragmentation because of the low ion intensity. As a control, we used a strong constitutive promoter for glutamine synthase to drive the expression of *cyp128* and found WT levels of SMK. For all future experiments, we used *Rv2269c* as the promoter for the *cyp128* complement strain (*cyp128::cyp128*).

We created an *rv2269c* deletion strain (*rv2269c*) in *M. tuberculosis* to confirm that it was not essential to SMK biosynthesis. To make the deletion strain, we replaced from nucleotides 94 to 280 with a hygromycin cassette. The hygromycin cassette was inserted in the same orientation as *cyp128* and *stf 3*, instead of in the opposite orientation as is usually done. The promoter for hygromycin drove the transcription of *cyp128* and *stf 3*, leading to increased levels of mRNA (data not shown) and resulted in increased levels of SMK (Figure 3B). The increased production of SMK in the *rv2269c* mutant enabled us to study the result of increased SMK production in our experiments.

Using the SMK mutants, we wanted to study its role in *M. tuberculosis* biology. We observed that *cyp128*, *stf 3*, and *rv2269c* showed no in vitro growth phenotype (Figure

S3B and ref 6). Previous analyses of SMK suggested that the sulfated variant is primarily situated in the outer cell envelope,⁶ unlike menaquinone, which is located in the plasma membrane.¹⁵ We confirmed this by the fractionation of the *M. tuberculosis* cell wall using hexanes, which selectively removes surface lipids from the covalently attached cell wall lipids.^{16,17} The majority of SMK was found in the hexanes fraction with minimal amounts detectable in the remaining cell pellet (Figure 3C). Despite having increased levels of SMK overall, the *rv2269c* mutant had an accumulation of SMK in the cell pellet, but cell surface levels remained similar to those found in WT (Figure 3C). This observation suggests that the exporting of SMK to the outer envelope is via active transport and is not mediated simply by passive diffusion from the cell interior.

To determine if SMK plays a role in the cell wall integrity, we subjected cells to chemical oxidative stress (H₂O₂, HClO₃, and NO), detergent stress (SDS), and cell wall biosynthesis inhibitors (isoniazid, ethambutol, and ethionamide) and measured the effects of these treatments on viability. Under all conditions, the SMK mutants showed no difference in survival from WT (Table S1), indicating that SMK does not play a role in the cell wall integrity.

Although SMK is not necessary for cell wall integrity, we hypothesized that this metabolite may play a role in the regulation of *M. tuberculosis* respiration. Menaquinone is essential to *M. tuberculosis* viability because of its role in the electron transport chain. Levels of menaquinone have been implicated in the activation of genes necessary for entry into and exit from an anaerobic culture.^{18–20} Mycobacteria primarily utilize menaquinone-9(II-H₂) (MK-9(II-H₂), Figure 1B), which has the second isoprene unit saturated. Analogue MK-9 (Figure S7), which has all isoprene units unsaturated, is found at lower levels than MK-9(II-H₂).¹¹ Enzyme MenJ that is responsible for converting MK-9 to MK-9(II-H₂) was recently identified in *M. tuberculosis*.²⁰ When MenJ is deleted in *M. smegmatis*, the bacteria increase the synthesis of MK-9 and utilize 3 times less oxygen than WT. Furthermore, when *M. tuberculosis* growth was inhibited using a menaquinone biosynthesis inhibitor under aerobic conditions, an analogue of MK-9 rescued the growth better than an analogue of MK-9(II-H₂).¹⁸ Both studies support an important role for menaquinone, specifically MK-9, in regulating respiration.

Because menaquinone is the precursor to SMK, SMK biosynthesis could alter menaquinone levels, leading to changes in the respiration of *M. tuberculosis*. We measured levels of MK-9 in the SMK mutants by LC-MS. We found that the *stf 3* mutant had significantly higher levels of MK-9 than WT, whereas the *stf 3::stf 3* strain partially complemented the phenotype (Figure 4). By contrast, both the *cyp128* mutant and *cyp128::cyp128* complement strains had WT levels of MK-9. We also measured levels of menaquinone in the *rv2269c* mutant that had significantly increased levels of SMK. Notably, the increased production of SMK did not significantly change menaquinone levels as compared to those in WT (Figure 4). The significant increase of MK-9 in the *stf 3* mutant suggests a regulatory link between menaquinone levels and SMK sulfotransferase *stf 3*.

The altered levels of MK-9 in the *stf 3* mutant suggested a role for SMK in the regulation of the electron transport chain in *M. tuberculosis*. We tested the susceptibility of the SMK

mutants to known inhibitors of the electron transport chain (scheme of the inhibitors and their targets, Figure S8). Each compound was serially diluted in media and inoculated with WT, the SMK mutants, or the complemented strains. Surprisingly, SMK mutants showed no distinguishing phenotype with respect to growth, ATP levels, or NADH/NAD⁺ ratio when treated with each compound. This suggests that SMK production does not alter *M. tuberculosis* growth or respiration rates under aerobic conditions.

Sulfated metabolites from other organisms, both bacterial and eukaryotic, often play roles in cell–cell communication or host–pathogen interactions.^{21,22} Sulfolipids from *M. tuberculosis* and the *M. avium* complex have known immunomodulatory effects.^{23,24} It is possible that SMK serves such a function for *M. tuberculosis*. Notably, *stf 3*, *cyp128*, and *rv2269c* have no obvious counterparts in mycobacteria outside the *M. tuberculosis* complex. Thus, the function of their product, SMK, may have a role specific for *M. tuberculosis* pathogenesis.

The earlier observation that *stf 3* is hypervirulent in mice supports the SMK-mediated modulation of *M. tuberculosis* virulence. The different levels of menaquinone in the *cyp128* and *stf 3* mutants suggest that *cyp128* may have a different phenotype in the mouse model of infection. We infected mice with the *cyp128* mutant in parallel with the *stf 3* mutant and their respective complement strains. BALB/c mice were infected via aerosol infection (200–300 CFU per lung) of each strain. Lungs were harvested after 3 weeks of infection, the first time point that a difference in growth between WT and the *stf 3* mutant was previously identified.⁶ Mice infected with the *cyp 128* mutant had significantly higher CFU in the lungs compared to WT, although not as many as the *stf 3* mutant (Figure 5). Both complemented strains showed WT levels of growth in the lungs.

Further studies are needed to understand why the SMK mutants have increased growth in mice. As we demonstrate here, SMK seems to play a negligible role in the growth or cell wall integrity of *M. tuberculosis* in vitro. Despite the difference in menaquinone levels between the *cyp128* mutant and the *stf 3* mutant, it is unlikely that the menaquinone levels can explain a change in respiration or growth rate to account for the increased number of bacteria in the lungs. Although this may contribute to the increase in growth of the *stf 3* mutant, it cannot account for the increase in growth of both mutants. An alternative hypothesis is that SMK alters the ability of the mouse to control bacterial growth during the acute phase of infection. As shown by Cambier et al., *M. tuberculosis* produces lipids to mask more immunostimulatory molecules on the surface.²⁵ SMK may be masking or altering the ability of macrophages to mount an effective response to *M. tuberculosis* infection. An alternative hypothesis is that SMK activates a specific immune response that is necessary for the control of *M. tuberculosis* growth. Further studies on the specific immune modulations of SMK are necessary to tease out the role of SMK. The elucidation of SMK biosynthesis and its role in *M. tuberculosis* pathogenesis adds to the repertoire of *M. tuberculosis* lipids known to have immunomodulatory effects in vivo.

METHODS

Bacterial Strains and Growth Media

The mycobacterial strains used in these studies were *M. tuberculosis* H37Rv and *M. smegmatis* mc²155. *M. tuberculosis* was grown in 7H9 (liquid medium) or 7H11 (solid medium) with 10% oleate/albumin/dextrose/catalase supplement, 0.5% glycerol, and 0.05% Tween 80 unless stated otherwise. *M. smegmatis* was grown in 7H9 (liquid) or 7H10 (solid) medium with 10% albumin/dextrose/catalase, 0.5% glycerol, and 0.05% Tween 80 unless stated otherwise. Media and supplements were from BD Biosciences. Antibiotics were used for selection at 20 $\mu\text{g}/\text{mL}$ kanamycin or 50 $\mu\text{g}/\text{mL}$ hygromycin for mycobacteria. Cloning and plasmid propagation were performed in *E. coli* TOP10 and XL-1 blue strains. *M. tuberculosis* genes were amplified from H37Rv genomic DNA. All *E. coli* cultures were grown in LB medium with 50 $\mu\text{g}/\text{mL}$ kanamycin or 100 $\mu\text{g}/\text{mL}$ hygromycin for selection.

Construction of *M. tuberculosis* Mutant Strains

The *cyp128* mutant strain was created by homologous recombination as previously described.²⁶ Briefly, specialized transduction phage phKMS109 (*rv2269c*) or phKMS110 (*cyp128*) was incubated with concentrated *M. tuberculosis* H37Rv for 4 h at 37 °C. Cells were then plated on 7H11 plates containing hygromycin. Colonies were picked and screened for gene disruption by PCR (Figure S2), which confirmed the replacement of 1279 bp of *cyp128* (amino acids 32–457) with a hygromycin resistance cassette. The *cyp128::cyp128* complementation strain was created by cloning the *cyp128* gene plus 333 bp upstream of the gene from *M. tuberculosis* strain H37Rv into mycobacterial expression vector pMV306, a derivative of the pMV361 vector²⁷ with a multiple cloning site in place of the expression cassette. The resulting plasmid was electroporated into *cyp128* cells, and transformants were selected on 7H11 kanamycin-containing plates.

Extraction and Mass Spectrometry Analysis of Lipids

Extraction and mass spectrometry analysis of lipids was performed as previously described.⁸ Briefly, for total lipid extracts (TLEs), mid-log-phase cultures of *M. tuberculosis* strains or *M. smegmatis* strains were washed and diluted in Tween-free media to an OD₆₀₀ of 0.2 and grown for two doublings. Cells were harvested via centrifugation, resuspended in 4 mL of 1:1 chloroform/methanol, and extracted overnight at RT. For surface lipid extractions, the pellet was resuspended in 2 mL of hexanes per 50 mL of culture and spun for 2 min at 3500 rpm. The upper organic phase was removed and added to an equal volume of 1:1 chloroform/methanol. The remaining cell pellet and aqueous phase were extracted with 4 mL of 1:1 chloroform/methanol per pellet overnight at RT. Cell debris was removed by centrifugation, and the supernatant was stored at –20 °C until analysis. All extractions were repeated in at least three independent experiments.

High-resolution FT-ICR mass spectra were obtained on an Apex II FT-ICR mass spectrometer equipped with a 7 T actively shielded superconducting magnet (Bruker Daltonics, Billerica, MA) as described previously.⁸ Briefly, samples were introduced into the ion source via direct injection at a rate of 2 $\mu\text{L}/\text{min}$. Ions were generated with an Apollo pneumatically assisted electrospray ionization source (Bruker Daltonics) operating in

negative ion mode and were accumulated in an rf-only external hexapole for 0.5–1 s before being transferred to the ICR cell for mass analysis. Mass spectra consisted of 512 000 data points and were an average of 50–100 scans. The spectra were acquired using XMASS version 7.0.8 (Bruker Daltonics). For accurate mass measurements, spectra were internally calibrated with known compounds.

Metabolic Labeling of *M. tuberculosis* and *M. smegmatis* with ³⁵S-Sulfate and Lipid Analysis by ThinLayer Chromatography (TLC)

M. tuberculosis or *M. smegmatis* strains were grown in 7H9 to late log phase. Two generations prior to labeling, strains were diluted to an OD₆₀₀ of 0.3. For ³⁵S-sulfate labeling, cells were resuspended at OD₆₀₀ ≈ 1 in 10 mL of PBS with 1% sodium acetate and 100 μCi of ³⁵S-sulfate (PerkinElmer). After overnight incubation, cell pellets were extracted with 1:1 chloroform/methanol as described above. Solvent was removed by evaporation, and the extracts were resuspended with 1:1 chloroform/methanol at 1/10 or 1/20 of the original volume. An equal volume of each fraction was spotted on silica plates (HPTLC silica gel 60, EMD Chemicals) and developed in 60:12:1 chloroform/methanol/water. Plates were analyzed by phosphorimaging (GE Biosciences Typhoon).

Quantification of Menaquinone Levels by LC-MS Analysis

Total lipid extracts from each strain were obtained as previously described. Using an authentic standard of menaquinone-9 (MK-9, Figure S3), we determined the unique fragmentation pattern used to identify MK-9 in complex samples for quantification by targeted metabolomics. We quantified ion counts for three independent transitions (*m/z* 785 to 109, 785 to 187, and 802 to 81; collision energy 12 V) from five replicates for each sample. All mass transitions showed the same trend in MK-9 levels for each *M. tuberculosis* strain. As an external standard, coenzyme Q₉ (CoQ₉, 1 ng) was added to total lipid extracts immediately after bacterial lysis. Each sample was filtered and transferred to a glass vial and stored at –80 °C until analysis. MS analysis was performed as previously described.²⁸ Briefly, an aliquot of the extract (10 μL) was analyzed using an Agilent G6430 QQQ instrument. Metabolite separation by liquid chromatography (LC) for lipophilic metabolites was achieved using a Gemini reverse-phase C5 column from Phenomenex. Mobile phase A consisted of 95:5 water/methanol, and mobile phase B consisted of 60:35:5 isopropanol/methanol/water. Formic acid (0.1%) was included to assist in ion formation in positive ionization mode. The flow rate for each run started at 0.1 mL/min with 0% B. At 5 min, the solvent was immediately changed to 60% B with a flow rate of 0.4 mL/min and increased linearly to 100% B over 15 min. This was followed by an isocratic gradient of 100% B for 8 min at 0.5 mL/min before equilibrating for 3 min at 0% B at 0.5 mL/min. Metabolites were detected using single reaction and were quantified by integrating the area under the curve and normalizing to the amount of external standard recovered and the OD₆₀₀ at the time of harvest. All values presented are averages of five replicates per strain with the standard deviation.

Minimum Inhibitor Concentration (MIC) Determination Using Chemical Inhibitors

M. tuberculosis was grown to mid log phase in 50 mL of 7H9 media in roller bottles. Clumps were removed by centrifugation, and the culture suspension was diluted to an OD₆₀₀

of 0.2. Two-fold serial dilutions of each chemical inhibitor were set up in 96 well plates, in concentrations starting with 4-fold over the literature MICs and in a total volume of 90 μL . Each well was inoculated with 10 μL of the designated strain in triplicate. Sterile PBS was added to the remaining wells. Plates were placed in a sealed Tupperware container containing damp towels to prevent evaporation. Plates were incubated for 7 days at 37 °C. Plates were fixed with 100 μL of 10% formalin in buffered PBS, and the cell density was quantified using a VersaMax UV/vis plate reader (Molecular Devices). MIC was determined by the concentration of treatment that inhibited 90% of growth compared to untreated conditions. Experiments were done in triplicate.

Mouse Infections

Female BALB/c mice were purchased from the Jackson Laboratory. Six week old mice were infected via the aerosol route. Bacteria were aerosolized by using the Inhalation Exposure System (Glas-col, Terre Haute, IN) to deliver 100 to 200 bacilli per mouse lung. To evaluate the initial inoculum, lungs from five mice were harvested 24 h after infection to determine the number of bacteria seeded. At 21 days after infection, bacterial numbers were enumerated by plating serial dilutions of lung homogenates from five mice for each group on 7H10-OADC. Colonies were counted after 21 days. The data represent one of two experiments.

Ethics Statement

All procedures involving the use of mice were approved by the University of California, Berkeley IACUC, the Animal Care and Use Committee (protocol number R353-1113B). All protocols conform to federal regulations, the National Research Council's *Guide for the Care and Use of Laboratory Animals*, and the Public Health Service's (PHS's) *Policy on Humane Care and Use of Laboratory Animals*.

Supplementary Material

Refer to Web version on PubMed Central for supplementary material.

Acknowledgments

We thank Drs. Sarah Gilmore, Jessica Seeliger, and Sarah Stanley for technical advice and their critical reading of the manuscript. This work was supported by National Institutes of Health grant R01 AI051622 and Howard Hughes Medical Institute to C.R.B., NCI R01 CA172667 to D.K.N., and R01 GM47356 to J.A.L.

ABBREVIATIONS

SMK	sulfomenaquinone
MIC	minimum inhibitory concentration
H₂O₂	hydrogen peroxide
HClO₃	chloric acid
NO	nitric oxide

SDS	sodium dodecyl sulfate
TLE	total lipid extract
TLC	thin layer chromatography

References

1. Mestre O, Hurtado-Ortiz R, Dos Vultos T, Namouchi A, Cimino M, Pimentel M, Neyrolles O, Gicquel B. High Throughput Phenotypic Selection of Mycobacterium tuberculosis Mutants with Impaired Resistance to Reactive Oxygen Species Identifies Genes Important for Intracellular Growth. *PLoS One*. 2013; 8:e53486. [PubMed: 23320090]
2. Stanley SA, Cox JS. Host-pathogen interactions during Mycobacterium tuberculosis infections. *Curr Top Microbiol Immunol*. 2013; 374:211–241. [PubMed: 23881288]
3. Jain M, Petzold CJ, Schelle MW, Leavell MD, Mougous JD, Bertozzi CR, Leary JA, Cox JS. Lipidomics reveals control of Mycobacterium tuberculosis virulence lipids via metabolic coupling. *Proc Natl Acad Sci U S A*. 2007; 104:5133–5138. [PubMed: 17360366]
4. Griffin JE, Pandey AK, Gilmore SA, Mizrahi V, McKinney JD, Bertozzi CR, Sassetti CM. Cholesterol catabolism by Mycobacterium tuberculosis requires transcriptional and metabolic adaptations. *Chem Biol*. 2012; 19:218–227. [PubMed: 22365605]
5. Lee W, VanderVen BC, Fahey RJ, Russell DG. Intracellular Mycobacterium tuberculosis Exploits Host-derived Fatty Acids to Limit Metabolic Stress. *J Biol Chem*. 2013; 288:6788–6800. [PubMed: 23306194]
6. Mougous JD, Senaratne RH, Petzold CJ, Jain M, Lee DH, Schelle MW, Leavell MD, Cox JS, Leary JA, Riley LW, Bertozzi CR. A sulfated metabolite produced by stf3 negatively regulates the virulence of Mycobacterium tuberculosis. *Proc Natl Acad Sci U S A*. 2006; 103:4258–4263. [PubMed: 16537518]
7. Mougous JD, Leavell MD, Senaratne RH, Leigh CD, Williams SJ, Riley LW, Leary JA, Bertozzi CR. Discovery of sulfated metabolites in mycobacteria with a genetic and mass spectrometric approach. *Proc Natl Acad Sci U S A*. 2002; 99:17037–17042. [PubMed: 12482950]
8. Holsclaw CM, Sogi KM, Gilmore SA, Schelle MW, Leavell MD, Bertozzi CR, Leary JA. Structural characterization of a novel sulfated menaquinone produced by stf3 from Mycobacterium tuberculosis. *ACS Chem Biol*. 2008; 3:619–624. [PubMed: 18928249]
9. ten Bokum AMC, Movahedzadeh F, Frita R, Bancroft GJ, Stoker NG. The case for hypervirulence through gene deletion in Mycobacterium tuberculosis. *Trends Microbiol*. 2008; 16:436–441. [PubMed: 18701293]
10. Cole ST, Brosch R, Parkhill J, Garnier T, Churcher C, Harris D, Gordon SV, Eiglmeier K, Gas S, Barry CE, Tekaia F, Badcock K, Basham D, Brown D, Chillingworth T, Connor R, Davies R, Devlin K, Feltwell T, Gentles S, Hamlin N, Holroyd S, Hornsby T, Jagels K, Krogh A, McLean J, Moule S, Murphy L, Oliver K, Osborne J, Quail MA, Rajandream MA, Rogers J, Rutter S, Seeger K, Skelton J, Squares R, Squares S, Sulston JE, Taylor K, Whitehead S, Barrell BG. Deciphering the biology of Mycobacterium tuberculosis from the complete genome sequence. *Nature*. 1998; 393:537–544. [PubMed: 9634230]
11. Collins MD, Pirouz T, Goodfellow M, Minnikin DE. Distribution of menaquinones in actinomycetes and corynebacteria. *J Gen Microbiol*. 1977; 100:221–230. [PubMed: 894261]
12. GALE PH, ARISON BH, TRENNER NR, PAGE AC, FOLKERS K. Characterization of vitamin K9(H) from Mycobacterium phlei. *Biochemistry*. 1963; 2:200–203. [PubMed: 13946232]
13. Johnston JB, Kells PM, Podust LM, Ortiz de Montellano PR. Biochemical and structural characterization of CYP124: a methyl-branched lipid omega-hydroxylase from Mycobacterium tuberculosis. *Proc Natl Acad Sci U S A*. 2009; 106:20687–20692. [PubMed: 19933331]
14. Shell SS, Wang J, Lapierre P, Mir M, Chase MR, Pyle MM, Gawande R, Ahmad R, Sarracino DA, Ioerger TR, Fortune SM, Derbyshire KM, Wade JT, Gray TA, Viollier PH. Leaderless Transcripts and Small Proteins Are Common Features of the Mycobacterial Translational Landscape. *PLoS Genet*. 2015; 11:e1005641. [PubMed: 26536359]

15. Lee SH, Sutherland TO, Deve R, Brodie AF. Restoration of active transport of solutes and oxidative phosphorylation by naphthoquinones in irradiated membrane vesicles from *Mycobacterium phlei*. *Proc Natl Acad Sci U S A*. 1980; 77:102–106. [PubMed: 6928606]
16. Goren MB. Sulfolipid I of *Mycobacterium tuberculosis*, strain H37Rv. I Purification and properties. *Biochim Biophys Acta, Lipids Lipid Metab*. 1970; 210:116–126.
17. Goren MB, D'Arcy Hart P, Young MR, Armstrong JA. Prevention of phagosome-lysosome fusion in cultured macrophages by sulfatides of *Mycobacterium tuberculosis*. *Proc Natl Acad Sci U S A*. 1976; 73:2510–2514. [PubMed: 821057]
18. Dhiman RK, Mahapatra S, Slayden RA, Boyne ME, Lenaerts A, Hinshaw JC, Angala SK, Chatterjee D, Biswas K, Narayanasamy P, Kurosu M, Crick DC. Menaquinone synthesis is critical for maintaining mycobacterial viability during exponential growth and recovery from non-replicating persistence. *Mol Microbiol*. 2009; 72:85–97. [PubMed: 19220750]
19. Honaker RW, Dhiman RK, Narayanasamy P, Crick DC, Voskuil MI. DosS responds to a reduced electron transport system to induce the *Mycobacterium tuberculosis* DosR regulon. *J Bacteriol*. 2010; 192:6447–6455. [PubMed: 20952575]
20. Upadhyay A, Fontes FL, Gonzalez-Juarrero M, McNeil MR, Crans DC, Jackson M, Crick DC. Partial Saturation of Menaquinone in *Mycobacterium tuberculosis*: Function and Essentiality of a Novel Reductase, MenJ. *ACS Cent Sci*. 2015; 1:292–302. [PubMed: 26436137]
21. Lerouge P, Roche P, Faucher C, Maillat F, Truchet G, Promé JC, Dénarié J. Symbiotic host-specificity of *Rhizobium meliloti* is determined by a sulphated and acylated glucosamine oligosaccharide signal. *Nature*. 1990; 344:781–784. [PubMed: 2330031]
22. Chapman E, Best MD, Hanson SR, Wong CH. Sulfotransferases: structure, mechanism, biological activity, inhibition, and synthetic utility. *Angew Chem, Int Ed*. 2004; 43:3526–3548.
23. Gilmore SA, Schelle MW, Holsclaw CM, Leigh CD, Jain M, Cox JS, Leary JA, Bertozzi CR. Sulfolipid-1 biosynthesis restricts *Mycobacterium tuberculosis* growth in human macrophages. *ACS Chem Biol*. 2012; 7:863–870. [PubMed: 22360425]
24. Khoo KH, Jarboe E, Barker A, Torrelles J, Kuo CW, Chatterjee D. Altered expression profile of the surface glycopeptidolipids in drug-resistant clinical isolates of *Mycobacterium avium* complex. *J Biol Chem*. 1999; 274:9778–9785. [PubMed: 10092667]
25. Cambier CJ, Takaki KK, Larson RP, Hernandez RE, Tobin DM, Urdahl KB, Cosma CL, Ramakrishnan L. *Mycobacteria* manipulate macrophage recruitment through coordinated use of membrane lipids. *Nature*. 2013; 505:218–222. [PubMed: 24336213]
26. Glickman MS, Cox JS, Jacobs WR. A novel mycolic acid cyclopropane synthetase is required for cording, persistence, and virulence of *Mycobacterium tuberculosis*. *Mol Cell*. 2000; 5:717–727. [PubMed: 10882107]
27. Stover CK, de la Cruz VF, Fuerst TR, Burlein JE, Benson LA, Bennett LT, Bansal GP, Young JF, Lee MH, Hatfull GF. New use of BCG for recombinant vaccines. *Nature*. 1991; 351:456–460. [PubMed: 1904554]
28. Nomura DK, Morrison BE, Blankman JL, Long JZ, Kinsey SG, Marcondes MCG, Ward AM, Hahn YK, Lichtman AH, Conti B, Cravatt BF. Endocannabinoid hydrolysis generates brain prostaglandins that promote neuro-inflammation. *Science*. 2011; 334:809–813. [PubMed: 22021672]

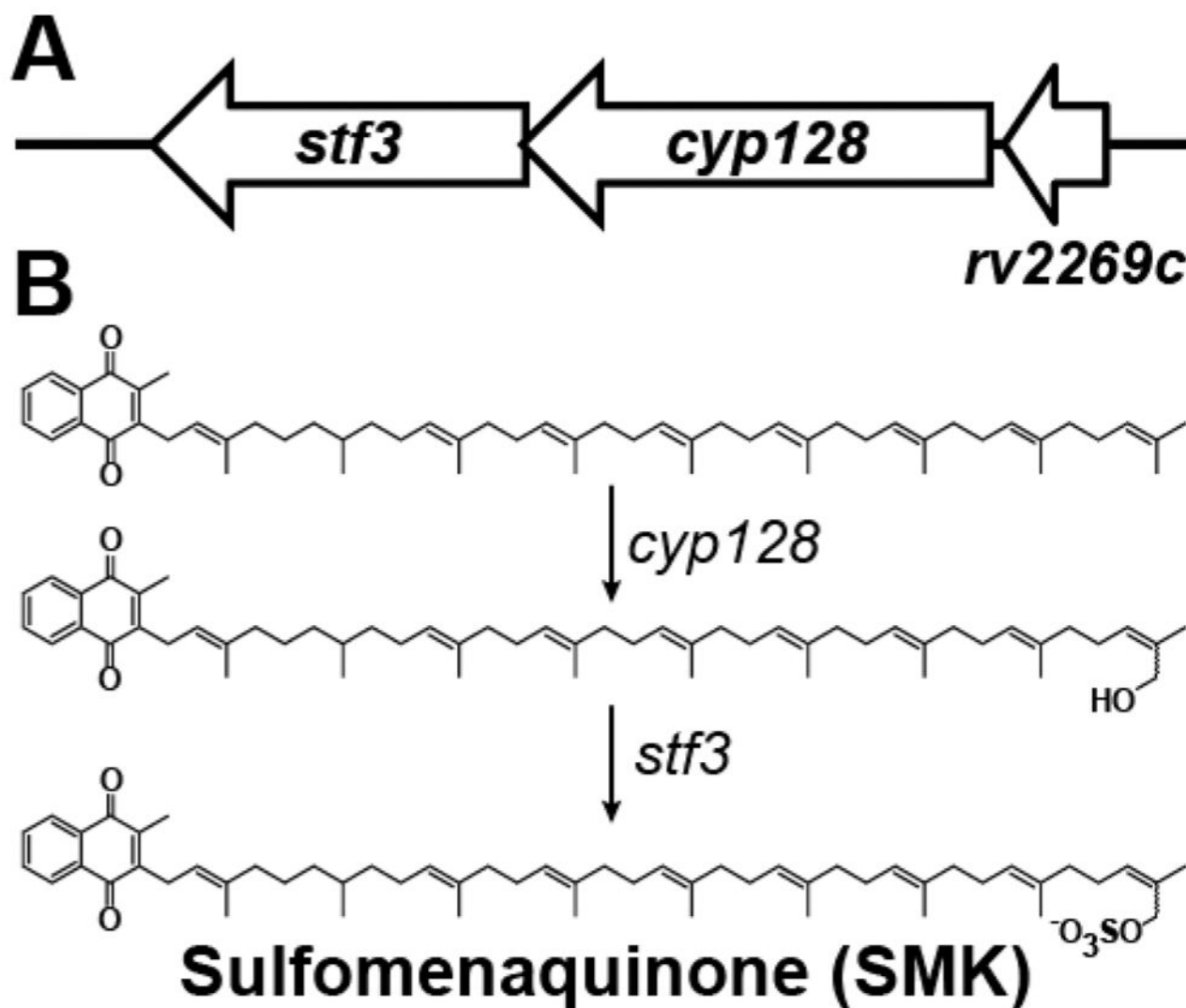


Figure 1.

Proposed SMK biosynthesis in *M. tuberculosis*. (A) The *stf3* operon contains three genes: *stf3* (*rv2297c*), the previously identified sulfotransferase required for SMK production; *cyp128* (*rv2298*), a putative cytochrome P450; and *rv2269c*, a conserved hypothetical protein of unknown function. The annotated start site of *stf3* is 6 bp before the annotated stop of *cyp128*. (B) Proposed biosynthesis of SMK. Menaquinone is hydroxylated by *cyp128* followed by *stf3* sulfation.

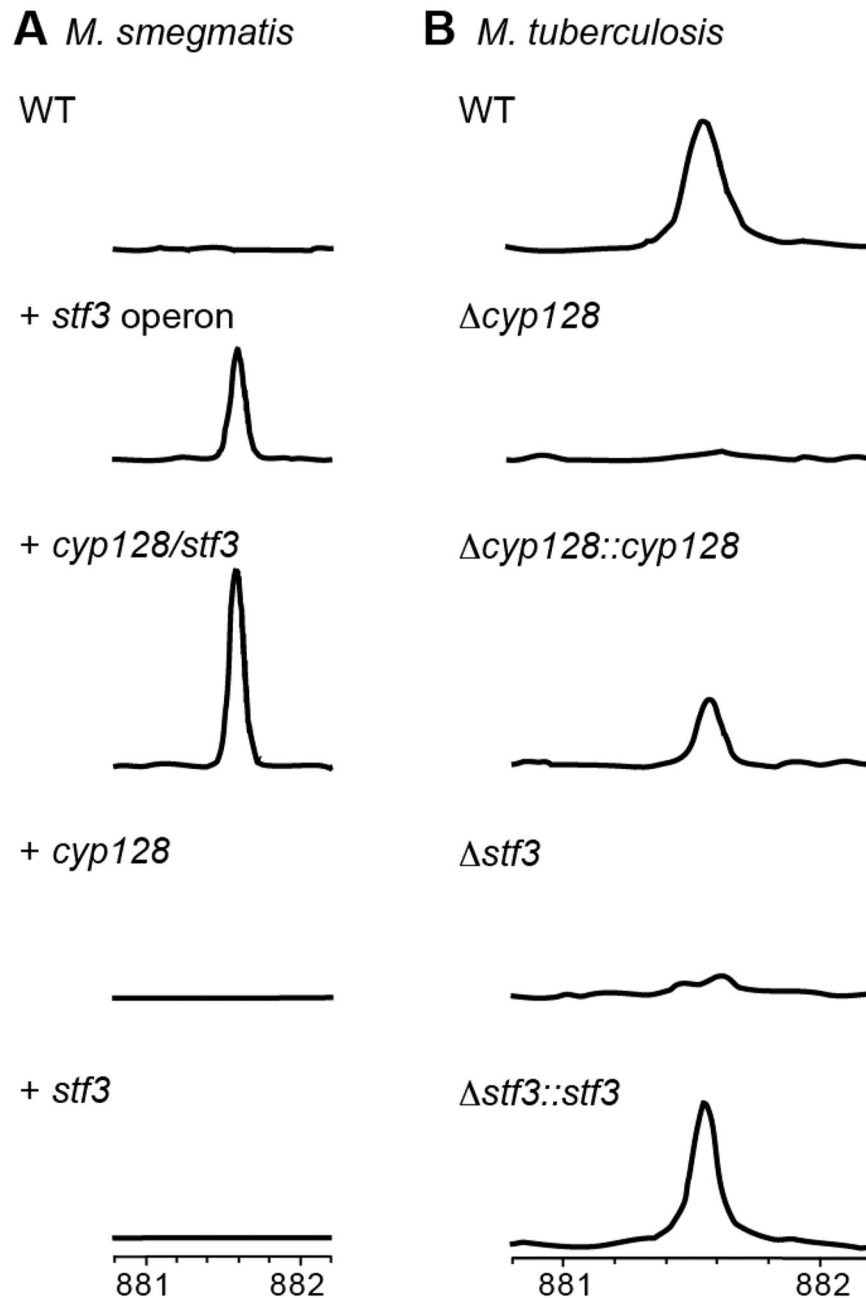


Figure 2. *cyp128* and *stf3* are required for SMK production. (A) Mass spectra of TLE from *M. smegmatis* strains expressing SMK biosynthetic genes. Only strains containing both *cyp128* and *stf3* produced SMK. The introduction of each of gene individually is not sufficient for SMK biosynthesis. (B) Mass spectra of TLE from *M. tuberculosis* WT and SMK deletion mutants. The deletion of *cyp128* from *M. tuberculosis* H37Rv (*cyp128*) resulted in a loss of SMK production similar to that of the previously characterized *stf3* deletion mutant (*stf3*). Complementation of *cyp128* (*cyp128::cyp128*) restores SMK production. A

representative scan from one experiment of FT-ICR mass spectra in region m/z 881– 882 is shown.

Author Manuscript

Author Manuscript

Author Manuscript

Author Manuscript

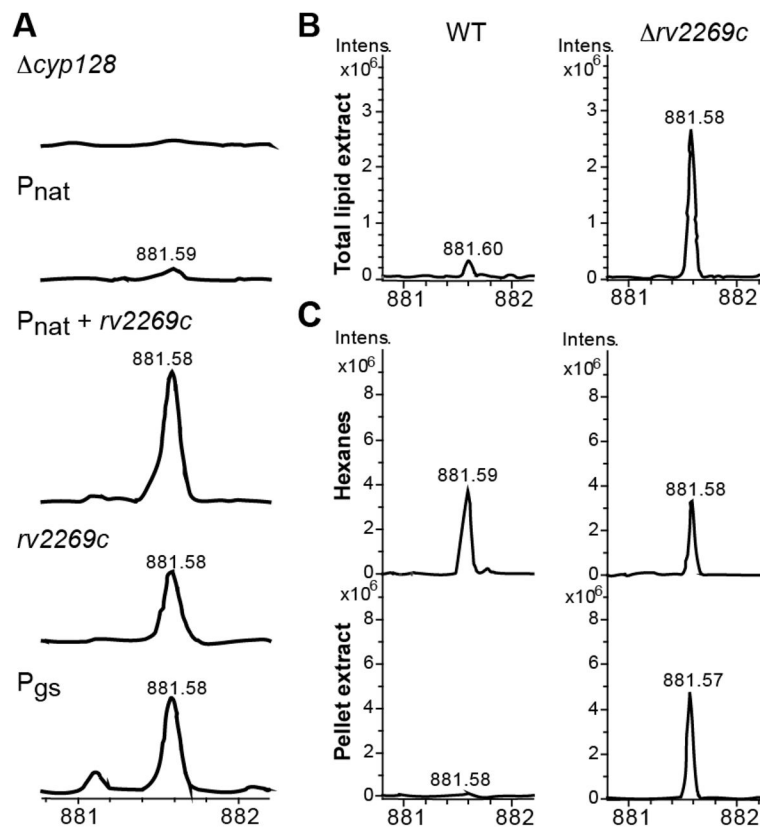


Figure 3. *Rv2269c* exhibits promoter activity. (A) Mass spectra of TLE from *cyp128* complementation strains with *cyp128* under the control of three different promoters. Only promoters containing *rv2269c* restored SMK production. The glutamine synthase promoter (P_{gs}) was used as a positive control. FT-ICR mass spectra scans in region *m/z* 881–882 are shown. (B) Comparison of mass spectra of TLE from WT *M. tuberculosis* and the *rv2269c* mutant. (C) Mass spectra of WT *M. tuberculosis* cell envelope fractionation are compared to the mass spectra from the *rv2269c* strain. Representative scans from one experiment of FT-ICR mass spectra scans in region *m/z* 881–882 are shown.

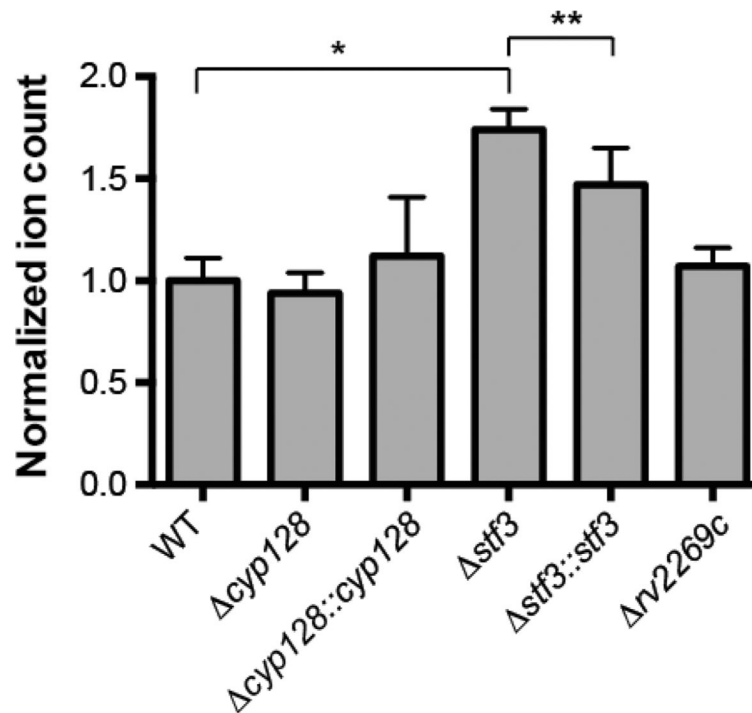


Figure 4. Levels of MK-9 as measured by the total ion count from targeted LC-MS/MS lipidomics from WT and SMK mutant strains from *M. tuberculosis*. Error bars indicate the standard deviation, $n = 5$. * $P < 0.01$ and ** $P < 0.05$.

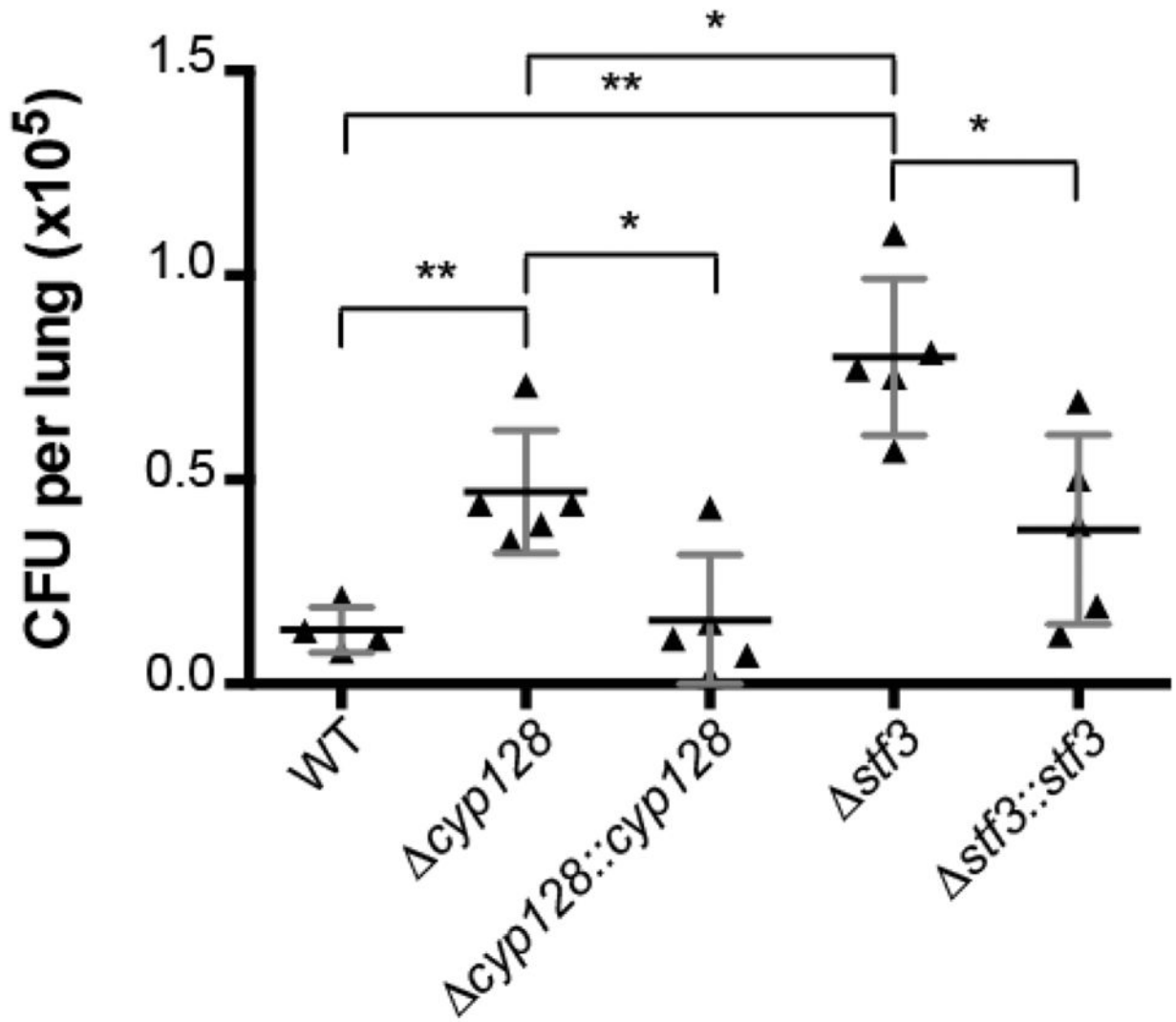


Figure 5. CFU from the lungs of mice. BALB/c mice were infected via aerosol infection with low-dose infection. Error bars indicate the standard deviation, $n = 5$. Data are shown from one of two experiments. * $P < 0.005$ and ** $P < 0.05$.